UNSYS digital

International Journal of Robotics and Mechatronics

Numerical and Experimental Investigation of Thermal Damage in Drilling of CFRP Composites

B. Shi[†], A . Sadek[†], M. Meshreki[†], H. Attia[†,§], J. Duquesne[‡]

[†]Aerospace Manufacturing, National Research Council Canada, Decelles Avenue, University of Montreal Campus, QC, Canada
[§]Department of Mechanical Engineering, McGill University, Canada
[‡]Airbus Operations S.A.S, Saint-Nazaire, France

***Abstract*—**Carbon fiber reinforced polymer (CFRP) composites are extensively used in aerospace applications due to their light weight and special strength. Drilling of holes is the most frequently used machining operation for CFRP composites. In the drilling process, heat conduction with the anisotropic thermal properties of CFRPs is a complex process that requires special considerations. In this study, a 3D finite element (FE) model is developed to predict the temperature fields in drilling of laminated composites, considering the unique features of CFRPs, i.e., the multi-ply structures and anisotropic thermal properties. The thermal energy is determined from the cutting forces and the cutting parameters. A novel methodology is proposed to determine the heat partition ratio between the CFRP and the drilling tool. It considers the tool speed and geometry, the material properties, as well as the tool coating. The predicted temperature and thermal damage are validated experimentally, which are in good agreement with the measurements.

***Keywords*—**Finite element modelling, drilling, CFRP composites, thermal analysis.

DOI: 10.21535/ijrm.v4i1.972

I. Introduction

In recent years, carbon fiber-reinforced polymer (CFRP) composites are extensively used in aerospace applications due to their light weight and special strength. Drilling of holes is the most frequently used machining operation for composites. One of the major defects in drilling of CFRP composites is thermal damage, which has significant effect on the mechanical properties of composite structures. The special feature of CFRPs, such as multi-ply structures and anisotropic material properties, causes the heat conduction process during the drilling of CFRPs to be very complex. Due to lack of an analytical solution, many studies have been conducted on modelling of machining of composites using FE analysis. These studies, however, focused on mechanical aspect, such as predictions of forces, torques, and delamination [1]-[5]. The study on modelling of thermal process during machining of CFRP is very limited. Diaz-Alvarezet et al [6] developed an axisymmetric 2D FE model to simulate the thermal process in drilling of CFRPs, which neglected the anisotropic thermal properties of CFRPs. Although it was a reasonable assumption for the woven carbon fiber laminated composite due to its semi-isotropic configuration, this 2D model cannot be applied in laminated composites with anisotropic configurations, such as uni-directional laminates. The objective of this study is to develop a generalized 3D FE thermal model for drilling of CFRPs, considering the process nonlinearity and the material removal by complex tool geometries. The multi-ply structures and anisotropic thermal properties of laminated composites were used in the model for temperature and thermal damage predictions. To validate the developed FE model, drilling tests were carried out using different types of drills under different drilling conditions. The predicted temperature and thermal damage were compared with the experimental measurements.

Corresponding author: Bin Shi (e-mail: bin.shi@cnrc-nrc.gc.ca).
This paper was submitted on April 1, 2017; revised on May 9, 2017; and accepted on August 31, 2017.

II. Thermal Load in Drilling of CFRP Composites

In drilling of CFRPs, the total work by torque (W_T) and thrust force (W_F) are converted to the heat generated at the tool-workpiece interface due to friction (Q), the energy required for breaking composites (E_b), and the kinetic energy of the chip (E_c). Therefore, the energy equilibrium equation is expressed by,

$$W_T + W_F = Q + E_c + E_b \tag{1}$$

Since the energy consumed by E_b and E_c is relatively small, all the work by W_T and W_F is assumed to be converted into heat Q [7]. Then, the average heat generation rate per area (heat flux), q, is written by,

$$q = \frac{dQ}{dt} = \frac{M\omega + F_a V_a}{S} \tag{2}$$

where M and F_a are the torque and the axial force, respectively; ω and V_a are the angular velocity and the axial velocity of the drill, respectively; S is the swept area of the cutting edges in one revolution. The values of M and F_a can be predicted using an analytical model [8]. In drilling of CFRP composites, the majority of heat generated in the process is transferred to the tool and the workpiece through the contact area between the tool and the workpiece. A very small portion of the heat is dissipated into the particle-like chip and the surrounding environment, which can be neglected [7]. If a heat partition

ratio, η, is defined as the percentage of the cutting energy that flows into the workpiece, then the heat flux applied on the workpiece, q_w, can be represented by,

$$q_w = \eta \times q \quad (3)$$

The heat partition ratio depends on the tool speed and geometry, as well as the thermal properties of the tool and the workpiece. In this study, a methodology is proposed to determine the heat partition ratio using a steady state FE thermal analysis. Figure 1 shows the geometrical models of a tool and a workpiece. The heat flux q_w is applied on the workpiece surface contacted with the tool tip (Figure 1 (b)), while the heat flux q_t is applied on the drill tip surface (Figure 1 (a)). In the two steady state FE models, heat convection boundary conditions are applied on the surfaces of the drill and the workpiece, respectively. Since the workpiece is stationary, the convective heat transfer coefficient of 20.0 W/m^2/K was used [9]. Convective heat transfer around a rotating object is a complex nonlinear process, which has been studied experimentally by several investigators [10]-[12]. To determine the convective heat transfer coefficient, it requires measurements of the surface temperature of the rotating body and the heat flux or the temperature gradient at its surface. However, it is very difficult to be determined experimentally because of the need for measuring the position and time dependent temperature field in a rotating part [13]. A simplified empirical model of the convective heat transfer coefficient is used in this study, which is a function of the surface speed of the rotating part [14],

$$h_c = 10.45 - V + 10V^2 \quad (4)$$

where h_c [W/m^2/K] is the convective heat transfer coefficient and V [m/s] is the surface speed of the drill. This empirical equation is applicable to the speed range of 2.0 to 20.0 m/s, which is equivalent to n=3,000 to 60,000 rpm for a tool diameter of D=6.0 to 12.0 mm.

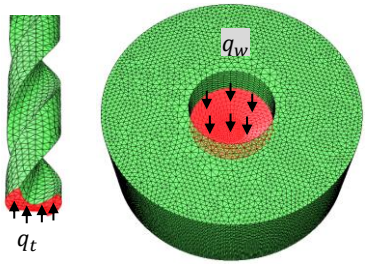

(a) Drill **(b) Workpiece**

Figure 1 Geometrical models used in the steady state FE analysis

Since the average temperatures of the contact surfaces on the tool and the workpiece should equal to each other when the drilling process reaches a thermal equilibrium state [15], the heat partition ratio η can be determined using the heat fluxes q_t and q_w that produce the same contact surface temperatures,

$$\eta = \frac{q_w}{q_w + q_t} \quad (5)$$

In the steady thermal analysis, carbide drills with diameters D=6.0, 9.0, and 12.0 mm and CFRP laminates with a configuration of $[0, 90]_{21}$ were used. The thermal conductivities of lamina along fiber, through-thickness, and transverse directions are k_{11}=5.0 (W/m/K), k_{22}=0.42 (W/m/K), and k_{33}= 0.42 (W/m/K), respectively. Figure 2 plots the dependence of the average surface temperatures on the applied heat fluxes for the CFRP (right side in Figure 2) and for the tool with a diameter D=6.0 mm and speed n= 6,000 rpm (left side in Figure 2). As shown in the figure, the average surface temperatures on the workpiece and the tool have linear relationships with the applied heat fluxes. Using Equation (5) the heat partition ratio was calculated to be 42%. Following the same approach, the heat partition ratios for different speeds were obtained.

Figure 3 shows the correlation of the heat partition ratio with the drill speed for D=6.0, 9.0 and 12.0 mm. It is shown that the heat partition ratio decreases with the speed increase. This is attributed to that high speed leads to more heat dissipating to the air through the tool and less heat flowing to the workpiece. The figure also shows that the heat partition ratio decreases with the tool diameter. This is due to that the larger tool has larger surface speed and contact area with the air, which results in more heat flowing to the tool side. It was found that the heat partition ratios for the speeds between 6,000 and 12,000 rpm are around 40% for D=6.0 mm, 37% for D=9.0 mm, and 30% for D=12.0 mm, which are within the range of 20-50% reported in [6]. For carbide tools and CFRP composites, an empirical model of the heat partition ratio η with the drill diameter D (mm) and speed n (rpm) is obtained,

$$\eta = 0.451 - 1.26 \times 10^{-3}D^2 + 6.79 \times 10^{-3}D + 1.08 \times 10^{-10}n^2 - 4.96 \times 10^{-6}n \quad (6)$$

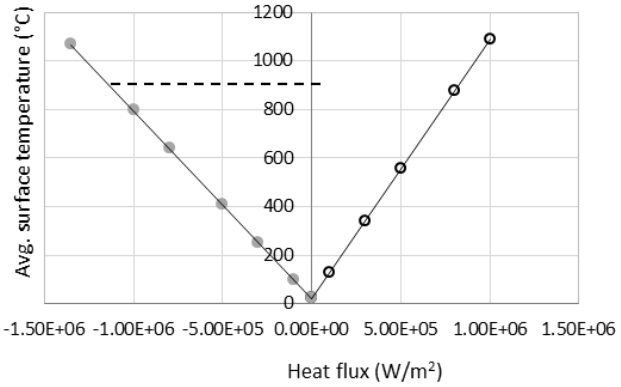

Figure 2: Dependence of the surface temperature on the heat flux (D=6.0mm, n=6000rpm)

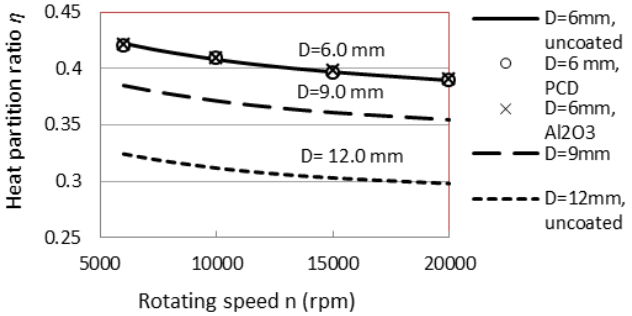

Figure 3: Heat partition ratio vs. rotating speed of carbide drills with diameter of 6.0mm (coated and uncoated), 9.0 mm (uncoated), and 12.0 mm (uncoated)

The effects of tool coating on the heat partition ratio were also investigated. Figure 3 shows the results for the drill diameter of D=6.0 mm with two types of coating, PCD (thickness 1.0 mm) and Al_2O_3 (thickness 0.2 mm). As shown in the figure, the effect of the coating on the heat partition ratio is insignificant and can be neglected.

III. 3D Finite Element Thermal Model

A 3D FE thermal model was developed to analyse the transient heat transfer process in drilling of CFRP composites. The 3D heat transfer process is governed by,

$$k_x \frac{\partial^2 T}{\partial x^2} + k_y \frac{\partial^2 T}{\partial y^2} + k_z \frac{\partial^2 T}{\partial z^2} + q = \rho c \frac{\partial T}{\partial t} \qquad (7)$$

where, k_x, k_y, k_z are the thermal conductivities of CFRP composites in the three directions, respectively; T, ρ and c are temperature rise, density and specific heat capacity of CFRP composites, respectively.

To reduce computation time by two orders of magnitude, the drill is not physically modelled in the FE analysis. A continuous layer removal approach is used to simulate the drilling process, as shown in Figure 4. The geometries of removed layers are determined by the profile and the location of the drill tip. The ply of CFRP laminates is also modelled. The anisotropic thermal properties for each ply are defined using its local coordinate system, whose orientation is determined by the CFRP configuration. The local (1-2-3) and the global (x-y-z) coordinate systems used in the model are shown in Figure 4. The numbers of 1, 2, and 3 of the local coordinate system represent the fiber, the through-thickness and the transverse directions, respectively. Figure 4 (a) shows an example of the local coordinates of Ply 1 and Ply 2, which indicates the fiber directions of the two plies have a 90° difference. This agrees with the CFRP configuration of $[0, 90]_{21}$.

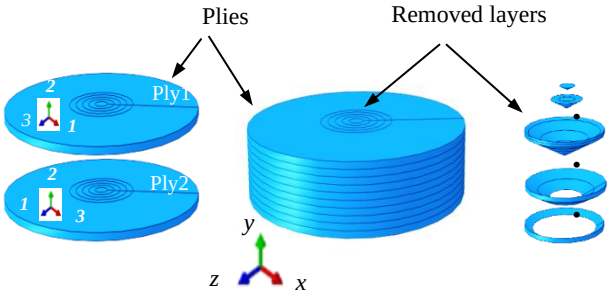

(a) Ply (b) 3D geometry c) Removed layer

Figure 4: CFRP laminates geometry with plies and removed layers

The thermal load defined in Section 2 is applied on the top surface of each removed layers until the current layer is removed. Then the thermal load is applied on the next removed layer. After one layer is removed, the temperature field in the rest of the workpiece is retained as an initial thermal condition for the next analyses step. The convection boundary condition is also applied in the model, where it is exposed to the air. The convection coefficient of 20 W/m^2/K was used in the model.

IV. Experimental Validation and Discussion

To validate the developed 3D FE thermal model, drilling experiments were carried out on a 5-axis machining center. An infrared camera (FLIR A20) was used to record the temperature field on the bottom surface of the CFRP plate through an inclined mirror (TECHSPEC® gold plated mirror), as shown in Figure 5. The drilling force and torque signals were measured using a Kistler 9272 piezoelectric dynamometer.

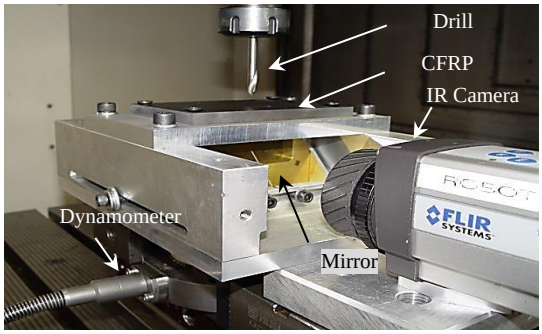

Figure 5 Experimental setup

Three types of drill (twist, multi-facet and candle stick) were used in the tests. The profiles and geometrical parameters of the drills are shown in Figure 6 and Table 1. The tool overhang and runout were 42 mm and 0.0127mm, respectively.

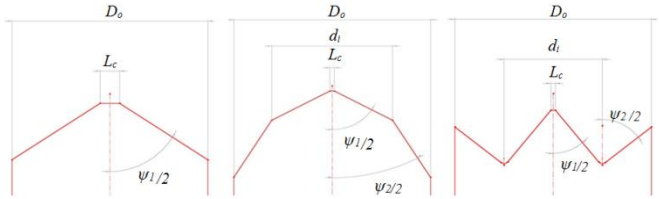

(a) Twist (b) Multi-facet (c) Candle stick

Figure 6 Profiles of the drills

Table 1 Geometrical parameters of the drills

Parameters	Twist	Multi-facet	Candle stick
D_0 (mm)	6	6	6
d_i/D_0	N/A	0.5	0.5
L_c(mm)	0.3	0.3	0.3
ψ_1 (deg)	90	120	80
ψ_2 (deg)	N/A	90	105

A. Temperature

Figure 7 (a) shows the comparison between the measured and predicted temperature fields when the twist drill tip just broke through the bottom of the CFRP plate. The cutting speed n=6,000 rpm and the feed f =0.08 mm/rev were used in this case. Figure 7 (b) shows the temperature distributions along a defined path indicated in Figure 7 (a). The results show that the predicted temperature distribution is in good agreement with the experimental measurement. The prediction error in the central portion is due to the effect of the chisel edge. However, this central portion will be removed in the drilling process. The error around in this portion does not affect significantly the prediction accuracy of thermal damage, which usually occurs

on the hole edge (shadowed area in **Figure 7 (b)**) when the temperature approaches the matrix deterioration temperature.

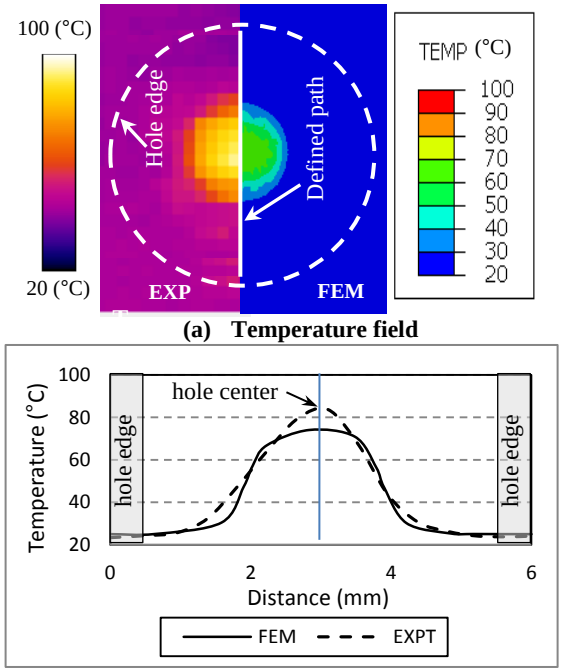

(a) Temperature field

(b) Temperature distribution

Figure 7 Temperature field and distribution on the exit plane as the twist drill tip breaks through the plate under the condition of *n*=6,000 rpm, *f*=0.08 mm/rev

The temperature at the exit hole edge was also investigated, where the maximum temperature usually happens in drilling of CFRP, as shown in Figure 8. Table 2 shows the comparison of the predicted and measured temperatures at the exit hole edge at different speeds of 5,000, 8,000 and 10,000 rpm (feed 0.08 mm/rev). The results show that the prediction errors are less than 10%.

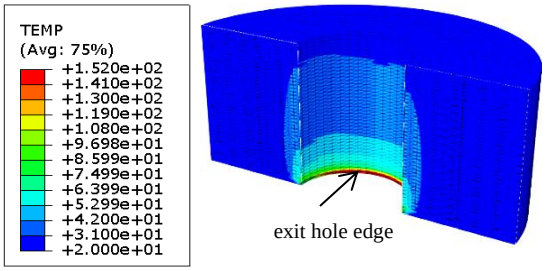

Figure 8 Temperature field at the exit hole edge (twist drill , *n*=5,000 rpm, *f*=0.08 mm/rev)

TABLE 2 COMPARISON OF THE PREDICTED AND MEASURED TEMPERATURES AT THE EXIT HOLE EDGE (TWIST DRILL)

Speed [rpm]	Feed [mm/rev]	Predicted *T* [°C]	Measured *T* [°C]	Prediction error
5,000	0.08	148	140	-5.7%
8,000	0.08	128	125	-2.4%
10,000	0.08	110	120	8.1%

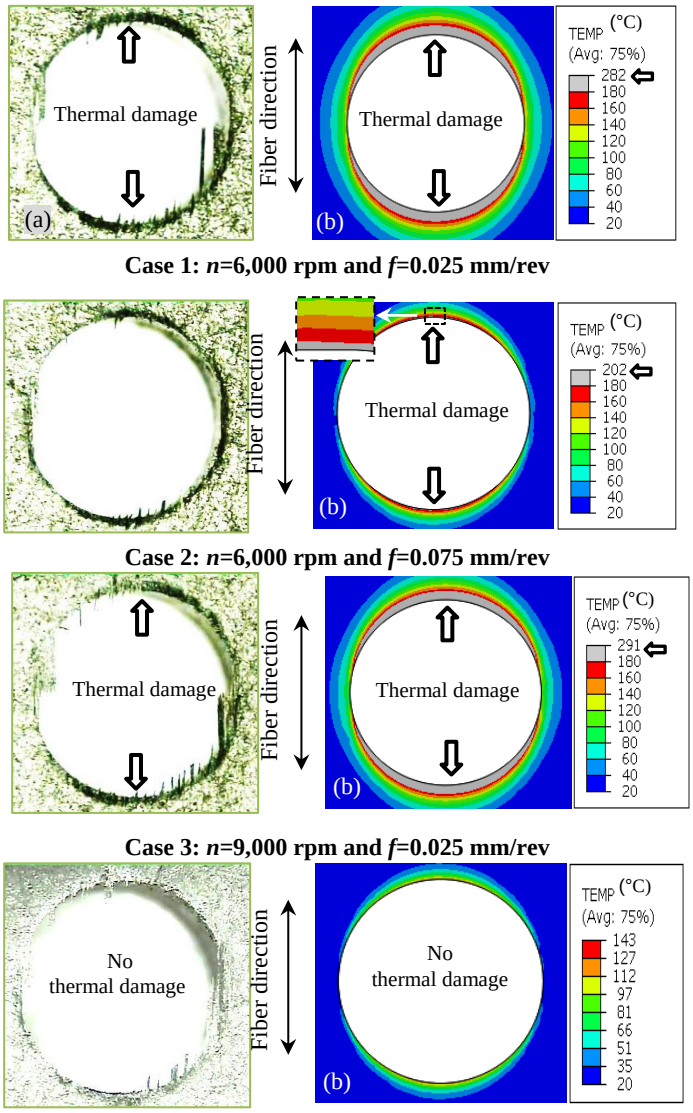

Figure 9 Predicted thermal damage and experimental observation for the twist drill. (a) Microscopic image; (b) Predicted temperature field at exit plane

B. Thermal damage

To demonstrate the validity of the model for prediction of thermal damage, four drilling cases using a twist drill with different speeds (6,000 and 9,000 rpm) and feeds (0.025 and 0.075 mm/rev) were investigated. Thermogravimetric analysis of the material used in this research showed that matrix deterioration temperature started at around 180°C. Above this critical temperature, matrix burnout will happen. The temperature of 180°C was used for predicting the occurrence of thermal damage. Figure 9 shows the comparison between the measured and the predicted thermal damage for the four cases. As shown in Case 1 (*n*=6,000 rpm and *f*=0.025 mm/rev), the predicted maximum temperature (peak temperature) of 282 °C is greater than the thermal damage temperature of 180 °C. The predicted thermal damage areas (the grey regions between 180 and 282 °C) are along the fiber direction, where the higher conductivity of the fibers allows faster heat flow. This strongly

agrees with the locations of the thermally damaged areas (the blackened region) from the experimental result. Case 2 has the same speed n=6,000 rpm, but larger feed f=0.075 mm/rev. In this case, the lower predicted peak temperature of 202 °C led to smaller thermal damage areas, compared to Case 1. This prediction is also in good agreement with the microscopic image given in the **Figure 9**, Case 2 (a). The larger feed has two different effects on the peak temperature. On one hand, it produced larger force and torque, which increases the thermal load. On the other hand, it led to less contact time between the tool and the workpiece, and then less heat dissipated to the workpiece. In Case 2, the latter effect dominated the heat conducting process that caused lower peak temperature. Case 3 has higher cutting speed n=9,000 rpm. A higher peak temperature of 291 °C was predicted. The predicted thermal damage areas also agree well with the experimental result. For Case 4 with n=9,000 rpm and f=0.075 mm/rev, the predicted peak temperature is 143 °C, which is lower than the thermal damage temperature of 180 °C. The thermal damage was not predicted for this case. The microscopic image also verified the validity of the prediction. The results of the four cases show that higher feeds lead to less thermal damage.

The developed 3D FE thermal model was also used to predict the thermal damages in drilling of CFRP when using a multi-facet and candle stick drills. **Figure 10** shows the comparison of the thermal damage predicted by the FE model and observed experimentally when using a multi-facet drill with D=6.0 mm, n=12,000 rpm and f =0.050 mm/rev. The prediction in **Figure 10 (b)** shows that the thermally damaged areas on the hole edge at exit are along the fiber direction with higher conductivity. This agrees very well with the locations in the experimental observation, as shown in **Figure 10 (a).**

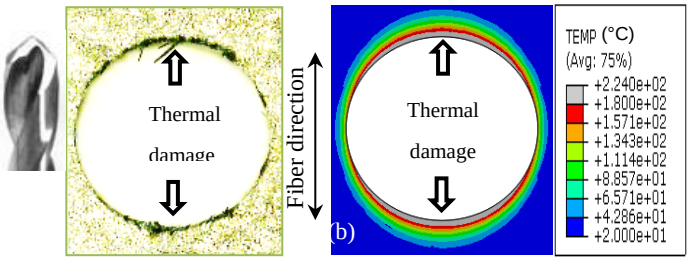

Figure 10 Predicted thermal damage and experimental observation for the multi-facet drill, n=12,000 rpm and f=0.050 mm/rev. (a) Microscopic image; (b) Predicted temperature field at exit plane

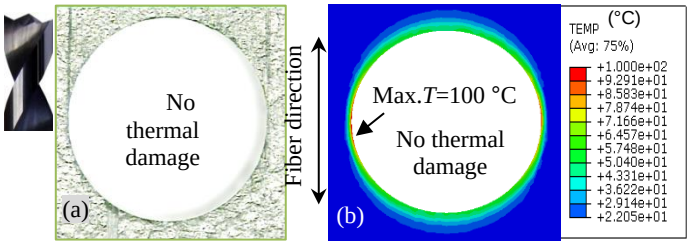

Figure 11 Predicted thermal damage and experimental observation for the candle stick drill D=6.0 mm, n=9,000 rpm and f=0.10 mm/rev. (a) Microscopic image; (b) Predicted temperature field at exit plane

Figure 11 shows a drilling case when using the candle stick drill with D=6.0 mm. The cutting condition for this case is the speed n=9,000 rpm and the feed f =0.10 mm/rev. As shown in **Figure 11 (b)**, the maximum predicted temperature at the exit surface is around 100 ℃. This temperature is much less than the thermal damage temperature of 180 ℃, indicating no thermal damage at exit for this case. This prediction agrees well with the experimental result given in **Figure 11 (a)**.

V. Conclusions

A novel 3D FE thermal model was developed in this paper to predict temperature fields in drilling of laminated composites. This model considers the multi-ply structures and anisotropic thermal properties of the CFRP composites. The drilling process was simulated using continuous layer removal of material. The thermal load applied on the workpiece was calculated based on the cutting energy and the heat partition ratio. A methodology was firstly proposed to determine the heat partition ratio between the CFRP workpiece and the drill, considering the tool speed, the material properties, tool coating, as well as the tool and workpiece geometries. An empirical model of the heat partition ratio η with the drill diameter D (mm) and speed n (rpm) for carbide tools and CFRP composites is propose. The heat partition ratio decreases with the tool diameter and speed increase. It was found that the heat partition ratios for the speeds between 6,000 and 12,000 rpm are around 40% for D=6.0 mm, 37% for D=9.0 mm, and 30% for D=12.0 mm. The effect of the tool coating on the partition ratio can be neglected. The predicted temperature fields and thermal damage areas were validated experimentally. The predictions were in good agreement with the experimental measurements. The results show that higher feeds lead to less thermal damage. The proposed model provides reliable predictive capability for process optimization and tool design in drilling of CFRP composites.

Acknowledgements

This work was conducted under the support of the Structure, Materials and Manufacturing Laboratory (SMM) of the National Research Council of Canada (NRC), and Airbus Airbus Operations S.A.S, which the authors greatly appreciate.

References

[1] Dandekar, C.R., and Shin, Y.C., "Modeling of machining of composite materials: A review." *International Journal of Machine Tools and Manufacture*, 57, pp.102–121, 2012. CrossRef

[2] Durao, L.M.P., Moura, M.F.S.F., and Marques, A.T., "Numerical simulation of the drilling process on carbon/epoxy composite laminates." *Composites: Part A*, 37, pp. 1325–1333, 2002. CrossRef

[3] Singh, I,; Bhatnagar, N., and Viswanath, P., "Drilling of uni-directional glass fiber reinforced plastics: experimental and finite element study." *Materials and Design*, 29, pp. 546–553, 2008. CrossRef

[4] Isbilir, O., and Ghassemieh, E., "Finite element analysis of drilling of carbon fibre reinforced composites." *Applied Composite Material*, 19, pp. 637–656, 2012. CrossRef

[5] Feito, N., Lopez-Puente, J., Santiuste, C., and Miguelez, M.H., "Numerical prediction of delamination in CFRP drilling." *Composite Structure* , 108, pp. 677–683, 2014. CrossRef

[6] Diaz-Alvarez, J., Olmedo, A., and Santiuste, C., Miguélez, H.; "Theoretical estimation of thermal effects in drilling of woven carbon fiber composite." *Materials*, 7, pp. 4442-4454, 2014. CrossRef

[7] Bono, M., and Ni, J., "A model for predicting the heat flow into the workpiece in dry drilling." *Journal of Manufacturing Science and Engineering*, 124, pp.773-777, 2002. CrossRef

[8] Sadek, A, Shi, B., Meshreki, M, Duquesne, J, and Attia, M.H., "Prediction and Control of Drilling-induced Damage in Fibre-reinforced Polymers Using a New Hybrid Force and Temperature Modelling Approach." *CIRP Annals - Manufacturing Technology*, Vol. 64 (1), pp. 89–92, 2015.

[9] Shi, B., Attia, H., and Tounsi, N., "Identification of material constitutive laws for machining-Part I: An analytical model describing the stress, the strain, the strain rate, and the temperature fields in the primary shear zone in orthogonal metal cutting." *ASME Journal of Manufacturing Science and Engineering*, 132/051008, pp. 1-11, 2008.

[10] Kops, L., and Arenson, M., "Determination of convective cooling conditions in turning." *CIRP Annals – Manufacturing Technology*, 48, pp. 47-52, 1999.

[11] Ozerdem, B., "Measurement of convective heat transfer coefficient for a horizontal cylinder rotating In quiescent air." *Int. Comm. Heat Mass Trans*, 27, pp. 389–395, 2000. CrossRef

[12] Elghnam, R. I., "Experimental and numerical investigation of heat transfer from a heated horizontal cylinder rotating in still air around its axis." *Ain Shams Engineering Journal*, Vol. 5 (1), pp. 177–185, 2014. CrossRef

[13] Attia, H., Joseph, P.M., and M'Saoubi, R., "Determination of convective heat transfer from rotating workpieces in dry and laser-assisted turning processes." *Advances in Materials & Processing Technology Conference*, Atlantis The Palm, Nov. 17-20, 2014, Dubai, United Arab Emirates.

[14] Glenn Elert, "The Physics Hypertextbook." [online]. Available: http://physics.info/, 1998.

[15] Shaw, M.C., *Metal Cutting Principles*. Oxford University Press, 1984.